International Journal of Pharmaceutics 420 (2011) 304–312

Contents lists available at SciVerse ScienceDirect

International Journal of Pharmaceutics

journal homepage: www.elsevier.com/locate/ijpharm

Liposome formulated with TAT-modified cholesterol for improving brain delivery and therapeutic efficacy on brain glioma in animals

Yao Qin[a,c], Huali Chen[a], Qianyu Zhang[a], Xiaoxiao Wang[a], Wenmin Yuan[a], Rui Kuai[a], Jie Tang[a], Li Zhang[a], Zhirong Zhang[a], Qiang Zhang[d], Ji Liu[b,**], Qin He[a,*]

[a] Key Laboratory of Drug Targeting and Drug Delivery Systems, Sichuan University, #17 Section 3, Renmin Nan Road, Chengdu Municipality 610041, Sichuan Province, PR China
[b] West China School of Preclinical and Forensic Medicine, Sichuan University, #17 Section 3, Renmin Nan Road, Chengdu Municipality 610041, Sichuan Province, PR China
[c] Taiji Group, #38 Huanglong Road, Chongqing Municipality 401147, PR China
[d] State Key Laboratory of Natural and Biomimetic Drugs, School of Pharmaceutical Sciences, Peking University 100191, PR China

ARTICLE INFO

Article history:
Received 28 June 2011
Received in revised form 29 August 2011
Accepted 11 September 2011
Available online 16 September 2011

Keywords:
TAT
Cholesterol
Doxorubicin
Brain delivery
Blood–brain barrier

ABSTRACT

The treatment of central nervous system diseases such as brain glioma is a major challenge due to the presence of the blood–brain barrier (BBB). A cell-penetrating peptide TAT (AYGRKKRRQRRR), which appears to enter cells with alacrity, was employed to enhance the delivery efficiency of normal drug formulation to the brain. Targeting liposomal formulations often apply modified phospholipids as anchors. However, cholesterol, another liposomal component more stable and cheaper, has not been fully investigated as an alternative anchor. In our study, TAT was covalently conjugated with cholesterol for preparing doxorubicin-loaded liposome for brain glioma therapy. Cellular uptake by brain capillary endothelial cells (BCECs) and C6 glioma cells was explored. The anti-proliferative activity against C6s confirmed strong inhibitory effect of the liposomes modified with doxorubicin-loaded TAT. The bio-distribution findings in brains and hearts were evident of higher efficiency of brain delivery and lower cardiotoxic risk. The results on survival of the brain glioma-bearing animals indicate that survival time of the glioma-bearing rats treated with TAT-modified liposome was much longer than in the other groups. In conclusion, the potency of the TAT-modified liposome to enter the BBB appears to be related with the TAT on the liposome's surface. The TAT-modified liposome may improve the therapeutic efficacy on brain glioma *in vitro* and *in vivo*.

1. Introduction

In brain tumors, common approaches to enhance drug concentration in the brain involve craniotomy-based drug delivery, such as local intracerebral implants, or disruption of the blood–brain barrier (BBB) by infusing hyperosmotic solution or vasoactive agent prior to systemic administration of the drug (Petri et al., 2007). Being highly invasive, these approaches are the most appropriate for short-term treatments, where a single or infrequent exposure to the drug is required. Though the invasive therapy may notably cut down the tumor cell burden, chemotherapy is not yet up to the task of two further orders of magnitude reduction in tumor cell numbers (Huynh et al., 2006). Biochemical and delivery challenges hinder the development of effective brain tumor drug therapies. Efficacy of the chemotherapy of brain pathologies is often impeded by insufficient drug delivery across the BBB (Takasato et al., 1984). Nearly 98% of small molecules and 100% of large molecules are prevented from being uptaken by BBB (William and Pardridge, 2005).There were several transport mechanisms at the BBB, including paracellular aqueous pathway, transcellular lipophilic pathway, specific receptor-mediated endocytosis, and absorptive endocytosis (Roney et al., 2005; Begley, 2004). Absorption-mediated transcytosis is triggered by an electrostatic interaction between the positively charged moiety of the peptide and the negatively charged plasma membrane surface region (Kumagai et al., 1987; Pardridge et al., 1989; Terasaki et al., 1989; Tamai and Tsuji, 1996). One of the cell-penetrating peptides, TAT, is the transactivating protein of the human immunodeficiency virus type-1, which is essential for viral replication (Banks et al., 2005). It can be reduced to a cluster of basic amino acids containing six arginine and two lysine residues within a linear sequence of amino acids. Their cationic charges facilitate the interaction with the normally negatively charged BBB, triggering permeabilization of the

* Corresponding author at: West China School of Pharmaceutics, Sichuan University, #17 Section 3, Southern Renmin Nan Road, Chengdu Municipality 610041, Sichuan Province, PR China. Tel.: +86 28 85502532; fax: +86 28 85502532.
** Corresponding author at: West China School of Pharmaceutics, Sichuan University, #17 Section 3, Southern Renmin Nan Road, Chengdu Municipality 610041, Sichuan Province, PR China.
E-mail addresses: liuji6103@163.com (J. Liu), qinhe@scu.edu.cn, qinhe317@126.com (Q. He).

0378-5173/$ – see front matter © 2011 Elsevier B.V. All rights reserved.
doi:10.1016/j.ijpharm.2011.09.008

cell membrane via a receptor/transporter independent pathway, which results in endocytosis of the sequence (Derossi et al., 1996). No saturable component to transport was found for either the influx or efflux of TAT. TAT has been shown to carry heterologous proteins into several cell types (Fawell et al., 1994) and carry protein, nanoparticles and quantum dots across the BBB (Schwarze, 1999; Liu et al., 2008; Santra et al., 2005). Our previous study proved that the Rhodanmin-labeled TAT-modified liposomes bear strong transendothelial ability in an in vitro BBB model, and biodistribution test found accumulation of TAT-modified liposomes in great quantity in animal brains (Qin et al., 2011).

Doxorubicin (DOX) is one of the most widely used anticancer agents. However, its clinical application is still limited by its deleterious side effects, including myelosuppression, gastrointestinal toxicity, and especially cardiotoxicity (Lee and Low, 1995). To avoid such complications, the use of liposomes as carriers for DOX has been recently explored in both animal and human trials (Mayer et al., 1989).

Active targeting liposomal formulations were nano-scale vesicles modified with ligand that can be used as chemical or biological drug carrying vesicles (Sharma and Sharma, 1997; Torchilin, 2005). In a previous study (Zhao et al., 2007), ligand was always modified on phospholipid such as DSPE. The DSPE introduces a negative charge onto the liposome surface, which may lead to additional plasma protein binding. It is not as chemically stable as cholesterol and is susceptible to degradation during storage. Cholesterol as a neutral anchor is cheap and more chemically stable. Thus, the replacement of DSPE with cholesterol is potentially more cost effective (Zhao et al., 2007).

To achieve high therapeutic efficiency of brain glioma, TAT-modified cholesterol was used to prepare the doxorubicin-loaded liposomes. *In vitro* and *in vivo* evaluations were made to examine the applicability of the TAT-modified liposomes for enhanced brain delivery.

2. Materials and methods

2.1. Materials

Doxorubicin was a gift from Haizheng Co. Ltd. Soybean phospholipids (SPC) were purchased from Shanghai Taiwei Pharmaceutical Co. Ltd., cholesterol (CHO) was purchased from Bio Life Science & Technology Co. Ltd., Shanghai, PR China. NH_2-PEG_{2000}-Mal and $mPEG_{2000}$-NH_2 was purchased from Jenkem Technology (Beijing, China). TAT peptide with terminal Cysteine (Cys-AYGRKKRRQRRR) was synthesized according to the standard solid phase peptide synthesis by Chengdu Kai Jie Bio-pharmaceutical Co. Ltd. (Chengdu, China). The BCA protein assay kit was purchased from Pierce (USA). The other chemicals were obtained from commercial sources. The 1,1′-dioctadecyl-3,3,3′,3′-tetramethylindotricarbocyanine (DIR) was purchased from Biotium (USA).

Kunming mice and Wistar rats were purchased from the Experimental Animal Center of Sichuan University (China). All animal procedures were approved by Experimental Animal Administrative Committee of Sichuan University.

2.2. Synthesis of CHO-PEG_{2000}-TAT and CHO-$mPEG_{2000}$

Cholesteryl chloroformate was reacted with NH_2-PEG_{2000}-Mal (molar ratio = 2:1) in dry triethylamine (TEA) at room temperature in argon in the presence of 4-dimethylaminopyridine (DMAP) for about 4 h. When NH_2-PEG_{2000}-Mal disappeared on thin layer chromatography (TLC), the reaction mixture was filtered. The filtrate was evaporated in vacuum. The residue was purified on a silica–gel chromatography column (DCM:MeOH = 1:1) to afford CHO-PEG_{2000}-MAL. CHO-PEG_{2000}-Mal and Cys-TAT (molar ratio = 1:1.5) were reacted in the mixture of $CHCl_3$/MeOH (v/v = 2:1) on gentle stirring at room temperature over night. When CHO-PEG_{2000}-Mal disappeared on TLC, the mixture was evaporated in vacuum, the residue was re-dissolved with $CHCl_3$, the insoluble material was filtered, and the supernatant (CHO-PEG_{2000}-TAT) was evaporated again in vacuum and stored at −20 °C for later use.

CHO-$mPEG_{2000}$ was synthesized as described above with a minor modification. NH_2-$mPEG_{2000}$ was used to react with the cholesteryl chloroformate instead of NH_2-PEG_{2000}-Mal.

2.3. Preparation of liposomes

Doxorubicin-loaded liposomes were prepared by remote loading using an ammonium sulfate gradient (Haran et al., 1993; Lasic et al., 1995). Lipid compositions of the prepared liposomes were as follows: (1) conventional liposomes (DOX-LIP), SPC:CHO = 66:34 (total lipid content: 3 μmol/mL); (2) long circulating liposomes (DOX-LLIP), SPC:CHO:CHO-$mPEG_{2000}$ = 66:26:8 (total lipid content: 3 μmol/mL); (3) TAT-modified liposomes (DOX-TAT-LIP), SPC:CHO:CHO-$mPEG_{2000}$:CHO-$mPEG_{2000}$-TAT = 66:26:3:5 (total lipid content: 3 μmol/mL). Briefly, the lipids of each composition were dissolved in chloroform, dried into a thin film on a rotary evaporator, and then hydrated with 300 mM of ammonium sulfate solution. The liposomal solution was extruded five times through a polycarbonate filter of 400, 200, and 100 nm in pore size sequentially with an extruder (Avanti, USA). The free ammonium sulfate was removed by passing through a Sephadex G-50 column in 0.9% sodium chloride. Five milliliters of liposomal solution and 0.65 mg of doxorubicin were mixed, and then incubated at 60 °C for 20 min. The doxorubicin-loaded liposomes were stored at 4 °C for later use.

The free doxorubicin was removed by passing through a Sephadex G-50 column. The envelopment efficiency of the liposomes was measured at E_x = 470 nm and E_m = 590 nm, respectively on a spectrofluorimeter (RF-5301 fluorospectrophotometry, Shimadzu, Japan).

The mean diameters and zeta-potentials of DOX-LIP, DOX-LLIP, and DOX-TAT-LIP were measured by Malvern Zetasizer Nano ZS90 (Malvern Instruments Ltd., UK).

DIR-loaded liposomes were prepared to investigate the distribution of each liposome in the brains of mice. Various amounts of lipid materials and DIR were dissolved in chloroform. Chloroform was then removed by rotary evaporation. The obtained thin film was kept in vacuum for over 6 h to remove the residual organic solvent completely. The thin film was hydrated in 5% glucose solution (pH 7.2) at 37 °C for 1 h. It was then intermittently sonicated with a probe sonicator at 100 W for 50 s.

2.4. Aggregation characteristic of liposomes in presence of fetal bovine serum (FBS)

Liposomes were prepared as described in Section 2.3. In order to investigate the aggregation characteristic of DOX-TAT-LIP and other control groups, DOX-LIP, DOX-LLIP, and DOX-TAT-LIP were mixed with the same volume of PBS containing 50% FBS, respectively. The mixture solution was incubated at 37 °C for 1, 2, 4, 8, 24 h to evaluate the variations of the transmittance at 750 nm. The relative transmittance in relation to that in PBS was calculated to evaluate aggregation of liposomes in blood stream (Maeda et al., 2004).

2.5. In vitro release of doxorubucin from liposomes

In vitro release of doxorubicin from liposomes was investigated in saline (pH 7.4) and saline containing 50% FBS. Two milliliters of liposomal solution was mixed with the same volume of saline

(pH 7.4) and saline containing 50% FBS, sealed into dialysis tubes (MW 8000–14,000), and incubated in 40 mL of saline at 37 °C for 48 h in thermal bath on continuous stirring. At the predetermined time points, aliquots in the dialysis medium were withdrawn, and doxorubicin concentration was measured by spectrofluorimeter (RF-5301 fluorospectrophotometry, Shimadzu, Japan) at E_x = 470 nm, E_m = 590 nm. The cumulative release percentage (%) was indicated by dividing the cumulative amount of doxorubicin recovered in the dialysis medium with the total amount in the liposomes (Jung et al., 2010; Charrois and Allen, 2004).

2.6. Confocal laser scanning microscopy (CLSM)

The doxorubicin-loaded liposomes were prepared as described above. BCECs and C6s were plated on gelatin-coated cover slips in 6-well culture plates. Different groups of liposomes and free doxorubicin were added to the plates with final concentration of doxorubicin was 0.5 μg/mL. After incubation at 37 °C in 5% CO_2 for 1 h, 2 mL of 2 μg/mL DAPI was added for 5 min, and the cells were washed three times with cold PBS and fixed using 4% paraformaldehyde. The cover slips were mounted cell-side down and viewed with a Leica TCS SP5 AOBS confocal microscopy system (Leica, Germany).

2.7. Quantitative evaluation of cellular uptake

BCECs were plated on gelatin-coated 24-well culture plates and cultured for 48 h. The BCECs were incubated with free doxorubicin (DOX), DOX-LIP, DOX-LLIP and DOX-TAT-LIP, which were diluted with medium containing FBS to different final DOX concentrations (2.5 μg/mL, 5.0 μg/mL, 10.0 μg/mL) for 1 h at 37 °C. In a separate experiment where the effects of incubation time on liposomes cellular uptake were studied, the cells were incubated with DOX, DOX-LIP, DOX-LLIP, and DOX-TAT-LIP of a final concentration of 5.0 μg/mL at 37 °C for 1, 4 and 8 h. At the end of the incubation period, the cells were washed three times with cold PBS and incubated with 1 mL/well 1% Triton-X 100 at 37 °C for 20 min. 100 μL of the lysate was set aside for the test of total protein of cells with the BCA assay kit, and the rest was added an additional 2 mL of 1% Triton-X 100 each and subject to cell-associated fluorescence determination at E_x = 470 nm, E_m = 590 nm respectively on a spectrofluorimeter (RF-5301 fluorospectrophotometry, Shimadzu, Japan). The results were described as the uptake indices, which were expressed in fluorescence/μg of protein.

C6s were plated on gelatin-coated 24-well culture plates, and cultured for 24 h. DOX, DOX-LIP, DOX-LLIP, and DOX-TAT-LIP were incubated with the C6s as described above.

2.8. Anti-proliferative activity against C6 glioma cells

C6 glioma cells were seeded into 96-well culture plates at a density of 1×10^4 cells/well and grown at 37 °C in presence of 5% CO_2 for 24 h. DOX, DOX-LIP, DOX-LLIP, and DOX-TAT-LIP were diluted with FBS-free medium, and added into 96-well cultured plates, respectively. The final concentrations of doxorubicin were in the range from 3 to 48 μg/mL. Twenty-four hours later, the medium was evacuated. Fresh medium was added and cultured for another 24 h. Cytotoxicity was measured with microtiter tetrazolium (MTT) assay, and absorbance was read on a microplate reader at 570 nm. The cells blankly treated were evaluated as controls. The survival percentage was calculated by the following formula: Survival (%) = (A570 nm for treated cells/A570 nm for control cells) × 100, where A570 nm was the absorbance value. Each assay was repeated in triplicates (Xiong et al., 2005; Yang et al., 2009).

2.9. Ex vivo near-infrared (NIR) fluorescence imaging

For *in vivo* optical imaging, mice were injected intravenously via vena caudalis with DIR-loaded liposomes. *Ex vivo* NIR fluorescence imaging was performed 4, 12 and 24 h after probe injection. The animals were sacrificed by perfusion of sodium chloride (N.S) in the heart. The whole brains were removed and placed into a whole-mouse imaging system (Imaging Station IS2000MM, Kodak) equipped with a band-pass filter at 700 nm and a long pass filter at 730 nm. Images were captured by the CCD camera embedded in the imaging (Ntziachristos et al., 2003; Frangioni, 2003).

2.10. Quantitative study of distribution in brain and heart

All procedures of the *in vivo* studies were approved by Sichuan University Animal Ethics Experimentation Committee following the Act of People's Republic of China on Use of Experimental Animals.

The mice were randomly assigned into four groups with each group further divided into five subgroups according to different time points. DOX, DOX-LIP, DOX-LLIP, and DOX-TAT-LIP were injected via the tail veins, where each animal received a dose of doxorubicin at 2.5 mg/kg. At 0.5, 1, 2, 4, and 8 h after the injection, the animals were sacrificed by cervical dislocation. The hearts and brains were removed and flushed with water three times to remove the blood remains. The tissues were homogenized with double amount of phosphate buffer (pH 9.0). 10 μL of internal standard (1 mg/mL Doxorubicin) was added into 200 μL organ homogenate, and extracted with 1 mL mixture solution of methanol and chloroform (4:1). The mixture was vortexed for 5 min, and centrifuged at 10,000 rpm for 5 min. The supernatant was transferred to another centrifuge tube, and dried under air stream at room temperature. The dry residue was reconstituted with 50 μL of mobile phase. The solution was centrifuged at 12000 rpm for 10 min, and then 20 μL of the supernatant was injected into the HPLC system for analysis. A reversed-phase HPLC was employed for the determination of doxorubicin concentrations in the plasma and tissue samples. A HPLC (Alltech, IL, USA) system with a Diamonsil C_{18} column (200 mm × 4.6 mm, 5 μm), and a mixture of methanol–acetonitrile–0.01 mol/L diammonium hydrogen phosphate–glacial acetic acid (50:22:28:0.6) as mobile phase were employed for the *in vivo* studies. The column temperature was 35 °C (Han et al., 2005).

2.11. Effects on the survival of brain tumor-bearing animals

Wistar rats (8 weeks of age initially weighing 220–250 g) were housed under standard conditions with free access to food and water. The animals were deeply anaesthetized with Chloral Hydratel (i.p. 400 mg/kg). Through a midline sagittal incision a burr hole of 1.5 mm in diameter was drilled at a point 1 mm posterior to the right coronal suture and 3 mm lateral to the sagittal midline (Adam et al., 2006; Gu et al., 2007). Approximate 5×10^7 C6 glioma cells which in 10 μL serum-free 1640 medium was implanted at a depth of 5 mm from the brain surface into the right forebrain. The scalp incision was closed. At day 3, after tumor inoculation, the rats were randomly divided into five groups (10 rats per group). Animals in blank control group were administered with physiological saline. Animals in other four groups were treated with DOX, DOX-LIP, DOX-LLIP, and DOX-TAT-LIP via tail vein at a dose of 2.5 mg/kg of doxorubicin, respectively. Administration was continued on days 6 and 12. Ten rats were used for monitoring the survival curves (Petri et al., 2007; Brigger et al., 2004). The survival time was calculated from the day 0 since tumor inoculation to the day of death. Kaplan–Meier survival curves were plotted for each group.

3. Results and discussion

3.1. Construction of liposomes

This study aims to develop liposomes formulated with TAT-modified cholesterol for enhancing their brain delivery and therapeutic efficiency on brain glioma. As one of the liposome ingredients, cholesterol was electro-neutral and chemically stable. The cost of cholesterol is merely one hundredth of DSPE. As a result, replacing DSPE with cholesterol seems potentially more cost-effective. Having said that, we coupled the TAT in our study to prepare the TAT-modified liposomes. Poly(ethylene glycol) (PEG) has always been modified onto the surface of liposomes for improved pharmacokinetics (PK) after intravenous (i.v.) administration and minimizing their protein binding to escape the surveillance of reticuloendothelial system (RES) (Li and Huang, 2010). However, excessive PEG modified on the surface of the liposomes might restrict cellular uptake.

TAT peptide density appears to be an important factor in cellular delivery of very large structures, such as liposomes (Eguchi et al., 2001). In our previous study, we confirmed that coupling the TAT peptide to the outer surface of liposomes might strongly increase the binding of liposomes to cells. Yet excessive TAT hardly contributed to the cellular delivery. It might also bind with the protein in the serum, and lower the stability of the liposomes. As a result, 5% of CHO-PEG-TAT was modified on the liposome to achieve ideal cell uptake, while 3% CHO-mPEG$_{2000}$ was added to shield the TAT and enhance the stability of the liposomes in the serum (Qin et al., 2011).

The potential of TAT-modified liposome for brain delivery was previously demonstrated *in vitro*. TAT played a key role in the cellular uptake and the transendothelial process on BBB model *in vitro*. This internalization process met the active endocytosis pathway, which might be mediated via multiple pathways, including the clathrin mediated endocytosis and macropinocytosis. The cationic charges of the TAT peptide certainly play a key role in the uptake process (Vives et al., 1997a,b; Wender et al., 2000). Both the positive and negative charges might decrease the cellular uptake of TAT-LIP, and block the transport of the TAT-LIP on BBB model *in vitro*. This result confirmed that the absorptive endocytosis might be one of the mechanisms of TAT-LIP crossing the BBB. Whether there were other pathways needed to further research.

To construct the liposomal drug delivery system, we first conjugated PEG$_{2000}$ to the CHO, and then the TAT anchored to the distal end of PEG$_{2000}$. TOF MS ES+ confirmed the formation of CHO-PEG$_{2000}$-TAT (Mw observed = 4208, Mw calculated = 4233). CHO-mPEG$_{2000}$ was synthesized as described above. TLC showed a purity of CHO-mPEG >95%.

3.2. Characterization and stability of liposomes

In this study, DOX-LIP was a common control group without modification. The DOX-LLIP contained 8% of CHO-mPEG$_{2000}$. The density of PEG on its surface was the same with the TAT-LIP. The control group certified the superiority and inferiority of the PEG. For the three types of liposomes, the average particle sizes were less than 150 nm, and the PDI were less than 0.2. The values of charge distributed around the liposome vesicles were shown in Table 1. The DOX-LIP and DOX-LLIP were weakly negatively charged, while the DOX-TAT-LIP was positively charged. The envelopment efficiencies were all over 90%.

All the liposomes investigated *in vivo* were tested *in vitro* in terms of stability in the presence of 50% FBS, which simulated the physiological environment of blood *in vivo*. The variation in transmittance according to different incubation periods of different samples incubated in 50% FBS at 37 °C were shown in Fig. 1.

Table 1
Characters of liposomes ($n = 3$).

	DOX-LIP	DOX-LLIP	DOX-TAT-LIP
Size (nm)	166.1 ± 2.17	100.2 ± 1.23	105.1 ± 2.22
PDI	0.184 ± 0.017	0.161 ± 0.025	0.179 ± 0.042
Zeta (Mv)	−8.20 ± 0.98	−6.43 ± 0.78	22.87 ± 0.80
EE (%)	96.65 ± 1.30	97.96 ± 1.60	93.53 ± 0.37

The transmittance of all kinds of liposomes did not show any drastic increase, suggesting that all the liposomes did not generate large aggregation in blood stream within 24 h.

3.3. Release of doxorubicin from liposomes

Release properties of doxorubicin from different liposomes were investigated at 37 °C in saline and saline containing 50% FBS. As shown in Fig. 2, there was little release of doxorubicin from these three liposomes during 24 h in saline. On the other hand, the *in vitro* doxorubicin release from liposomes showed a comparatively gentle release profile in 50% FBS. However, the TAT might induce faster release than other two liposomes in 50% FBS. The reason might be that the protein in the FBS decreased the stability of the lipid bilayer, and the permeability of the liposome was increased. In the later process, the proteins were binding with the liposome and interrupting the release of the doxorubicin. The cumulative release of doxorubicin was almost the same for three liposomes either in saline or in saline containing 50%FBS. The cumulative doxorubicin release of each liposome was over 85% in saline, and over 60% in 50% FBS. There were no pronounced differences in doxorubicin release from each liposome at every time point. The TAT modified on the surface of the liposome did not change the release behavior of the liposome.

3.4. Cellular uptake

After 1 h of incubation, doxorubicin was localized in BCECs and C6s. The cell nucleuses were stained blue with DAPI. The red fluorescence could be found in the cell nucleus and cytoplasm. Among all the four kinds of groups, the internalization of liposomes modified with TAT by the BCECs and C6s was the most evident (Fig. 3). The strongest red fluorescence could be found in these two cells after treated with DOX-TAT-LIP indicated that the most of liposomes were delivered into the cells. The red florescence was mostly found in the cell nucleus and cytoplasm. The fluorescence exhibited by the BCECs and C6s treated with DOX, DOX-LIP and DOX-LLIP markedly decreased.

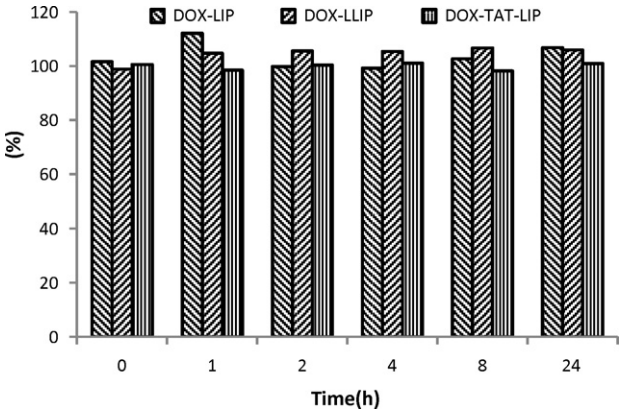

Fig. 1. Aggregation characteristic of each liposome. The prepared liposomes were incubated in 50% FBS at 37 °C for 1, 2, 4, 8 and 24 h. Transmittance of the solutions was measured at 750 nm. Relative transmittance was calculated against that in PBS (%).

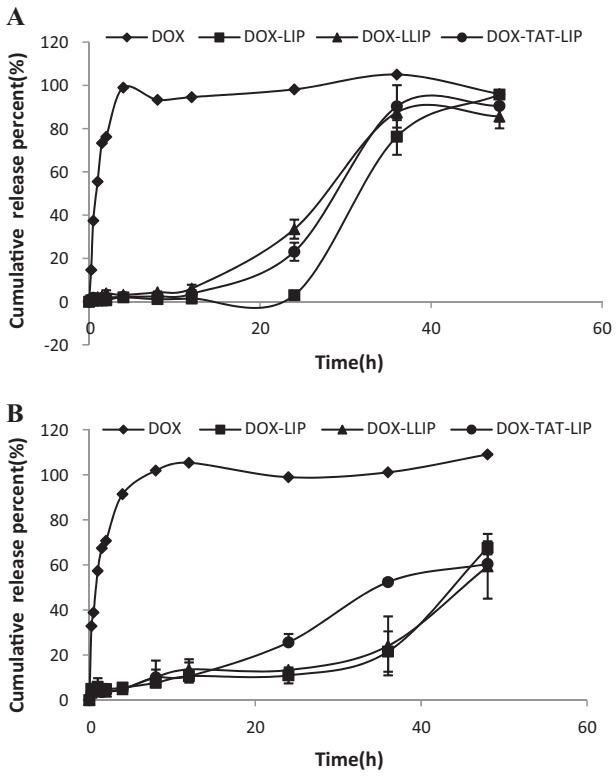

Fig. 2. Release profiles of doxorubicin from liposomes at 37 °C in (A) normal saline and (B) 50% FBS. Mean ± SD are shown ($n = 3$).

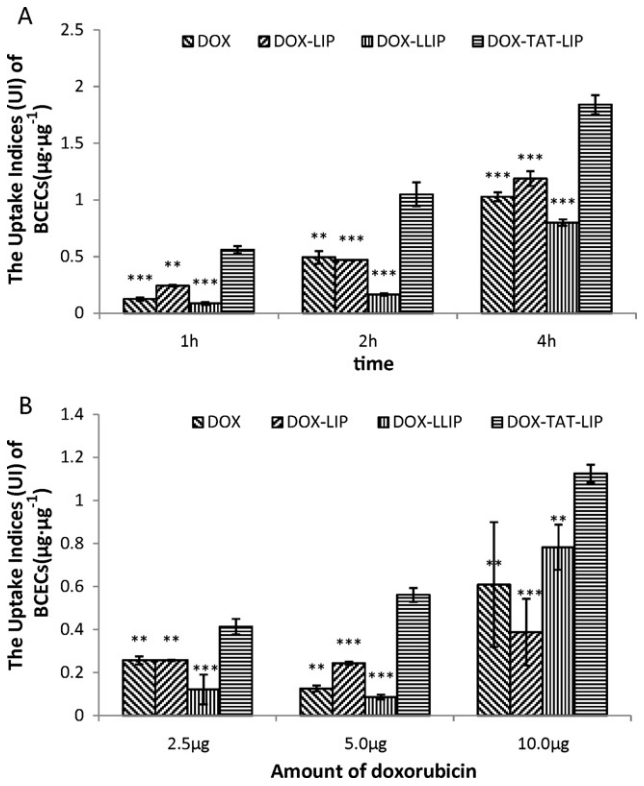

Fig. 4. Quantitative evaluation of cellular uptake by BCECs. Cellular uptake is expressed as uptake indices ($n = 3$). (A) Cellular uptake was measured 1, 4, and 8 h after treatment with different formulations with the same doxorubicin concentration. (B) Cellular uptake was measured 1 h after treatment with different formulations with different doxorubicin concentrations ($n = 3$). The data are presented as mean ± SD. $^{*}P < 0.05$; $^{**}P < 0.01$; $^{***}P < 0.001$; versus DOX-TAT-LIP.

The cellular uptake of each formulation by BCECs was also in a time-dependent manner within 8 h (Fig. 4A). The uptake indices of DOX-TAT-LIP were 3.45, 1.12 and 0.79 times higher than those of DOX; 1.31, 1.23, and 0.55 times higher than those of DOX-LIP; 5.46, 5.32 and 1.12 times higher than those of DOX-LLIP at 1, 4 and 8 h in the medium containing 10% FBS, respectively.

The uptake indices (Fig. 4B) of DOX-TAT-LIP were 0.61, 3.45 and 0.85 times higher than those of DOX; 0.61, 12.31, and 1.90 times higher than those of DOX-LIP; 2.41, 5.41 and 0.44 times higher than those of DOX-LLIP at 2.5, 5.0, and 10.0 μg of DOX in the medium containing 10% FBS, respectively.

The cellular uptake of each formulation by C6s was also in a time-dependent manner within 8 h (Fig. 5A). The uptake indices of DOX-TAT-LIP were 2.24, 1.30, and 1.68 times higher than those of DOX; 1.08, 0.74, and 1.62 times higher than those of DOX-LIP; 4.26, 1.56, and 2.25 times higher than those of DOX-LLIP at 1, 4, and 8 h in the medium containing 10% FBS, respectively.

The uptake of each formulation by C6s was in a concentration-dependent manner within 8 h (Fig. 5B). The uptake indices of TAT-LIP were 5.39, 2.24 and 1.30 times higher than those of DOX; 1.63, 1.08, and 0.74 times higher than those of LIP: 3.18, 4.26, and 7.75 times higher than those of LLIP at 2.5, 5.0, and 10.0 μg of DOX in the medium containing 10% FBS, respectively.

We can conclude that the cellular uptake of DOX-TAT-LIP was improved noticeably by TAT modification compared with unmodified LLIP and LIP. In our previous study (data not shown), the Rho-labeled liposomes had also been uptaken by BCECs efficiently.

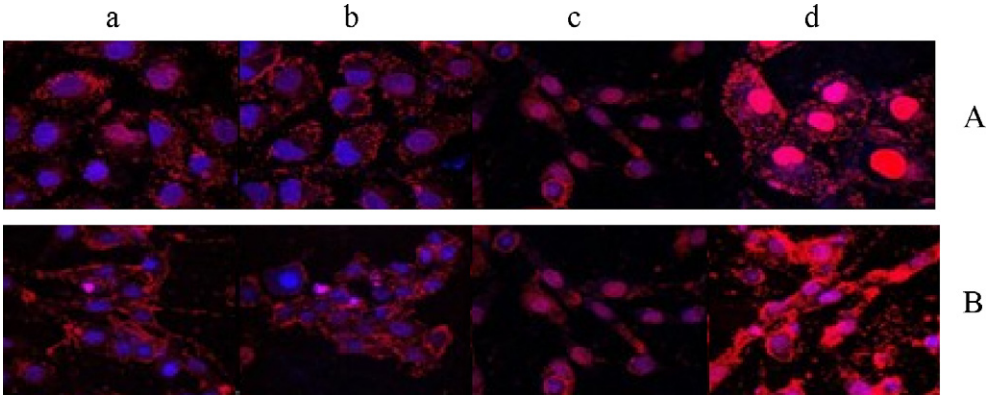

Fig. 3. Cellular uptake of doxorubicin-loaded liposomes by BCECs (A) and C6s (B) concentrations of liposomes in all samples were adjusted to 5 μg/ml of doxorubicin per well. For each line was (a) DOX, (b) DOX-LIP, (c) DOX-LLIP, and (d) DOX-TAT-LIP.

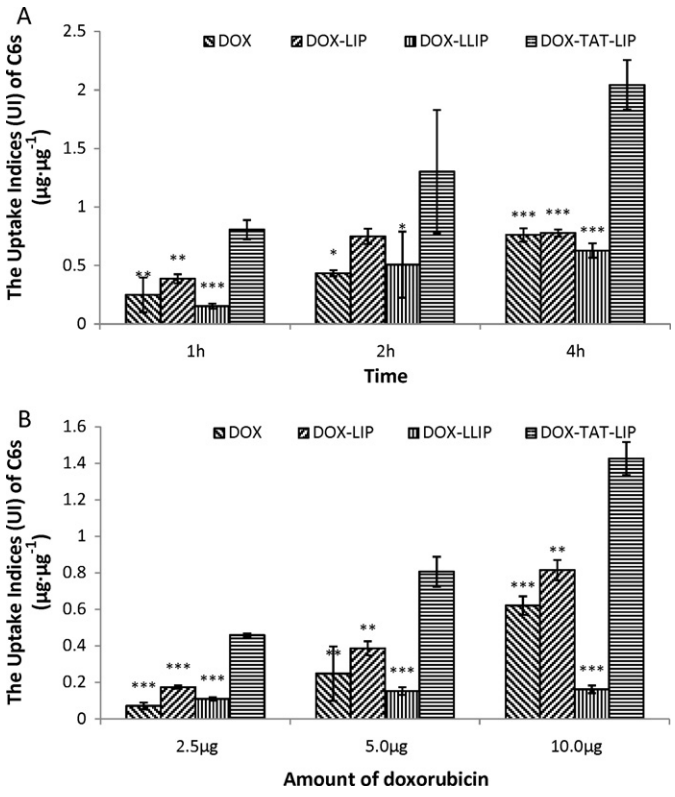

Fig. 5. Quantitative evaluation of cellular uptake by C6s. Cellular uptake is expressed as uptake indices ($n = 3$). (A) Cellular uptake was measured 1, 4, and 8 h after treatment with different formulations with the same doxorubicin concentration. (B) Cellular uptake was measured 1 h after treatment with different formulations with different doxorubicin concentrations ($n = 3$). The data are presented as mean ± SD. $^{*}P < 0.05$; $^{**}P < 0.01$; $^{***}P < 0.001$; versus DOX-TAT-LIP.

So, the TAT could not only deliver the carrier, but also the cargo into the cells. The uptake process showed a time-dependent manner. LLIP showed the poorest cellular uptake, which might be due to the presence of PEG in high density on the liposome. The PEG on the surface of the liposomes restricted the interaction between the LLIP and cellular membrane.

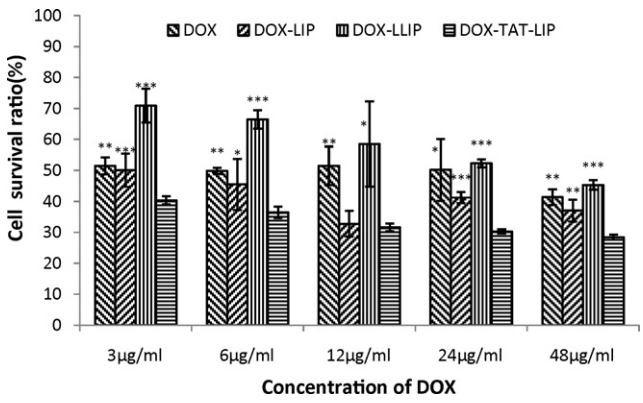

Fig. 6. Anti-proliferative effect by directly applying each formulation for 24 h. The data are presented as mean ± SD. $^{*}P < 0.05$; $^{**}P < 0.01$; $^{***}P < 0.001$ versus DOX-TAT-LIP.

3.5. Anti-proliferative effects on C6 glioma cells

Fig. 6 represents the anti-proliferative effect of each formulation on C6 glioma cells. The results from MTT assay showed that the DOX-TAT-LIP exhibited the strongest inhibitory effect on the proliferation of C6 glioma cells among all the other formulations under different concentrations. The IC_{50} values of DOX, DOX-LIP, DOX-LLIP, and DOX-TAT-LIP were 7.88, 1.63, 29.96, and 0.33 μg/mL, respectively. The IC_{50} value of TAT-LIP was 24.24 times lower than that of DOX. In comparisons between the drug-loaded liposomes, the IC_{50} value of DOX-TAT-LIP was 4.94, and 90.79 folds lower compared to DOX-LIP and DOX-LLIP, respectively, indicating that the anti-proliferative effect of the drug-loaded liposomes was markedly elevated by the modification with TAT.

3.6. Ex vivo near-infrared (NIR) fluorescence imaging

Recently, near-infrared (NIR) fluorescence imaging has emerged as a potential tool for imaging (Ntziachristos et al., 2003; Frangioni, 2003). In the NIR wavelength range of 700–900 nm, light penetrates relatively deep into the tissue. The NIR fluorescence imaging offers advantages such as nonradioactivity and high sensitivity compared

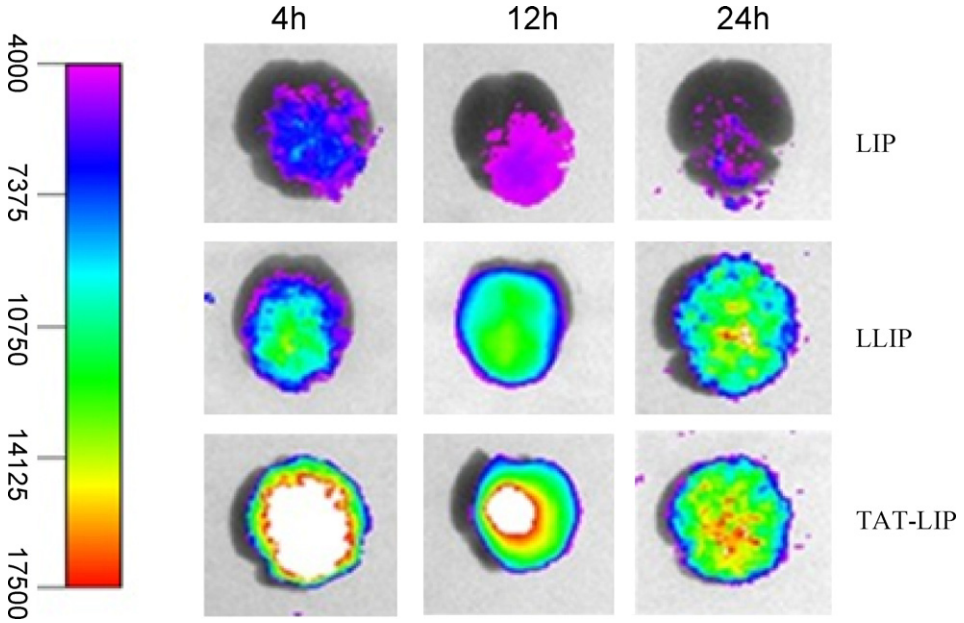

Fig. 7. *Ex vivo* imaging of brain given different DIR-loaded liposomes via tail vein.

with conventional techniques (Xu et al., 2007; Tromberg et al., 2008). After 4 h the injection, there was defined fluorescent signal in the brains of DIR-TAT-LIP group. However, the strong NIR fluorescent signal was observed coming from the brains of the mice injected intravenously with the DIR-TAT-LIP 12 and 24 h after injection. Weak signals exhibited in the brains of control animals treated with DIR-LIP and DIR-LLIP during the same period of time (Fig. 7). The LLIP might be more stable *in vivo,* and its circulating time might be longer than the LIP. So it might have more chance to contact with the BBB. That might be the reason that we found more fluorescence signals in LLIP group.

3.7. Distribution of different liposomes and free doxorubicin in mouse brains and hearts

The quantitative study of biodistribution could reveal the character of each formulation *in vivo* more precisely and literally. Doxorubicin distributed in brain and heart could be completely separated and detected under the selected analytical method, which could be validated by the standard curves (r of all tissues >0.995), and the recoveries were between 85% and 115% in all tested tissues. The concentrations of doxorubicin in the brain of TAT-LIP at 0.5, 1, 2, 4, 8 h were 3.05, 5.60, 1.80, 1.74, and 1.09 times higher than those of DOX; 3.38, 6.58, 2.16, 2.08, and 0.20 times higher than those of DOX-LIP; and 0.22, 0.73, 2.72, 10.49, and 0.45 times higher than those of DOX-LLIP (Fig. 8A). The concentrations of doxorubicin in the hearts of DOX-TAT-LIP at 0.5, 1, 2, 4, 8 h were much lower than those of free doxorubicin (Fig. 8B), which indicated that the distribution of doxorubicin in heart was decreased. The data had showed that the DOX-TAT-LIP accumulated the most in the brain of all within 8 h after the administration. The clinical application of doxorubicin is still limited by its deleterious side effects, especially for cardiotoxicity (Lee and Low, 1995). The concentration of DOX-TAT-LIP in the heart was lower that that of DOX. These data showed that the DOX-TAT-LIP could not only transport into the brain effectively, but also decrease the distribution of the doxorubicin in the heart.

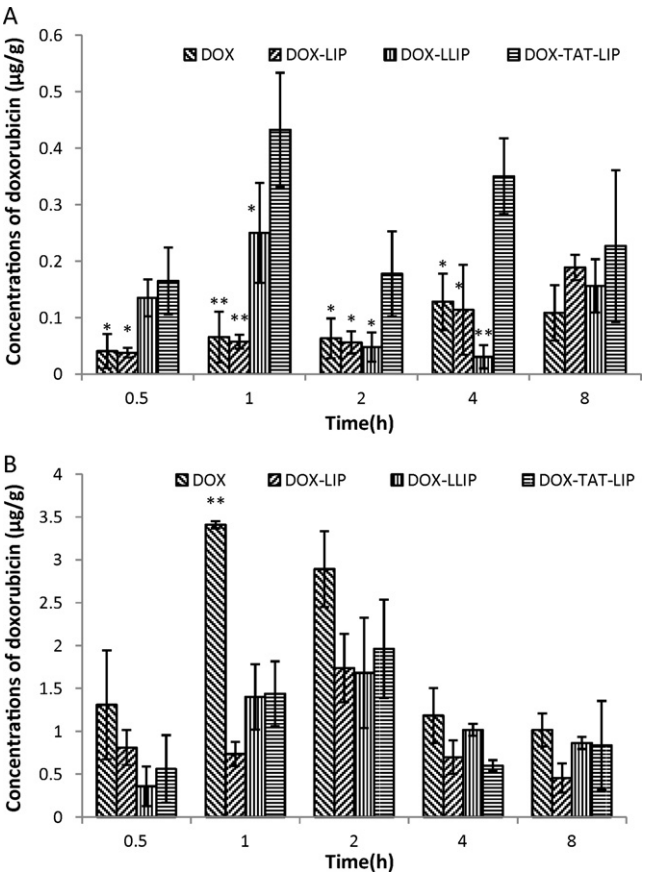

Fig. 8. Bio-distribution of each formulation in mice at different time points expressed as doxorubicin concentration in brain (A) and heart (B). The data are presented as mean ± SD. $^{*}P<0.05$; $^{**}P<0.01$; $^{***}P<0.001$ versus DOX-TAT-LIP.

3.8. Effects on survival of brain tumor-bearing animals

For defining the efficacy of the functionalized liposomes in animals, brain glioma-bearing rat models were applied. As shown in Table 2, the presence of TAT as well as the liposomes as a formulation parameter increased the therapeutic efficacy. The data in Table 2 focused on the short-term survival results. After the treatment, the median survival time of rats treated with DOX-TAT-LIP (89 days) was significantly longer than those of rats treated with physiological saline (54 days), DOX (32 days), DOX-LIP (53 days), and DOX-LLIP (69 days), respectively (Table 2). The Kaplan–Meier survival curves (Fig. 9) emphasized on the long-term survivors. It can be seen that DOX-TAT-LIP showed the best anti-tumor effects, endowing long-term remission to 40% of the animals. The DOX-LLIP produced single long-term survivor. The animals in other three groups were all dead within 100 days. Necropsy of the long-term survivors performed 100 days post tumor implantation revealed no signs of tumor growth.

At the initial days after the administration, some of the animals which were treated with doxorubicin solution refused to take food and water, moved slowly, developed hematuria and appeared lethargy, while the weight decreased rapidly. These might be caused by the side effects of the doxorubicin. As a result, the life span of animals treated with doxorubicin was slightly shorter than the N.S group. Survival curves, median survival time, and mean survival time showed that the DOX-TAT-LIP significantly enhance the therapeutic effect in the brain glioma-bearing Wistar rats, indicating that the TAT is able to increase the transport of the drug across the BBB and to improve the therapeutic effect on the brain glioma.

Table 2
Means and median for survival time ($n = 10$).

Group	Means	SD	95% Conf. interval (days)		Median	SD	95% Conf. interval [days]	
			Lower	Upper			Lower	Upper
N.S	53.500***	5.323	43.066	63.934	54.000***	3.162	47.802	60.198
DOX	42.600***	8.429	26.079	59.121	32.000***	3.162	25.802	38.198
DOX-LIP	57.500***	3.798	50.055	64.945	53.000***	2.635	47.835	58.165
DOX-LLIP	66.800**	9.401	48.260	85.340	69.000	22.136	25.614	112.386
DOX-TAT-LIP	79.400	8.351	63.872	94.928	89.000	20.555	48.713	129.287

$^{*}P<0.05$ versus DOX-TAT-LIP.
$^{**}P<0.01$ versus DOX-TAT-LIP.
$^{***}P<0.001$ versus DOX-TAT-LIP.

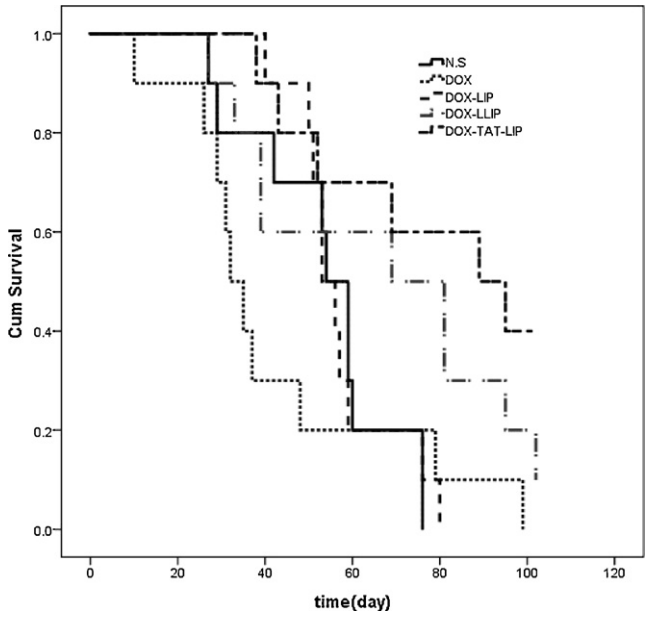

Fig. 9. Kaplan–Meier survival curves.

4. Conclusion

In conclusion, the *in vitro* and *in vivo* experimental data indicate that the TAT-modified liposomes may be a promising brain drug delivery system, which is capable of improving the therapeutic efficacy on brain glioma both *in vitro* and *in vivo*.

Acknowledgments

We are thankful for the financial support of the National Natural Science Foundation of China (30873166, 81072599), the State Key Program of National Natural Science Foundation of China (81130060) and the National Basic Research Program of China (2009CB903300).

References

Adam, J.F., Joubert, A., Biston, M.C., Charvet, A.M., Peoch, M., Le Bas, J.F., Balosso, J., Estève, F., Elleaume, H., 2006. Prolonged survival of Fischer rats bearing F98 glioma after iodine-enhanced synchrotron stereotactic radiotherapy. Int. J. Radiat. Oncol. Biol. Phys. 64, 603–611.

Banks, W.A., Robinson, S.M., Nath, A., 2005. Permeability of the blood–brain barrier to HIV-1 TAT. Exp. Neurol. 193, 218–227.

Begley, D.J., 2004. Delivery of therapeutic agents to the central nervous system: the problems and the possibilities. Pharmacol. Ther. 104, 29.

Brigger, I., Morizet, J., Laudani, L., Aubert, G., Appel, M., Velasco, V, Terrier-Lacombe, M.-J., Desma Jle, D., d'Angelo, J., Couvreur, P., Vassal, G., 2004. Negative preclinical results with stealth® nanospheres-encapsulated Doxorubicin in an orthotopic murine brain tumor model. J. Control. Release 100, 29–40.

Charrois, G.J.R., Allen, T.M., 2004. Drug release rate influences the pharmacokinetics, biodistribution, therapeutic activity, and toxicity of pegylated liposomal doxorubicin formulations in murine breast cancer. Biochim. Biophys. Acta 1663, 167–177.

Derossi, D., Calvet, S., Trembleau, A., Brunissen, A., Chassaing, G., Prochiantz, A., 1818. Cell internalization of the third helix of the Antennapedia homeodomain is receptor independent. J. Biol. Chem. 271, 8–18193.

Eguchi, A., Akuta, T., Okuyama, H., Senda, T., Yokoi, H., Inokuchi, H., Fujita, S., Hayakawa, T., Takeda, K., Hasegawa, M., Nakanishi, M., 2001. Protein transduction domain of HIV-1 TAT protein promotes efficient delivery of DNA into mammalian cells. J. Biol. Chem. 276, 26204–26210.

Fawell, S., et al., 1994. TAT-mediated delivery of heterologous proteins into cells. Proc. Natl. Acad. Sci. U.S.A. 91, 664–668.

Frangioni, J.V., 2003. *In vivo* near-infrared fluorescence imaging. Curr. Opin. Chem. Biol. 7, 626–634.

Gu, Y.-T., Zhang, H., xue, Y.-X., 2007. Dexamethasone enhances adenosine 5′-triphosphate-sensitive potassium channel expression in the blood–brain tumor barrier in a rat brain tumor model. Brain Res. 1162, 1–8.

Han, H.D., Lee, A., Song, C.K., Hwang, T., Seong, H., Lee, C.O., Shin, B.C., 2005. *In vivo* distribution and antitumor activity of heparin-stabilized doxorubicin-loaded liposomes. Int. J. Pharm. 313, 181–188.

Haran, G., Cohen, R., Barenholz, Y., 1993. Transmembrane ammonium sulfate gradients in liposomes produce efficient and stable entrapment of amphipathic weak bases. Biochem. Biophys. Acta 1151, 201–215.

Huynh, G.H., Deen, D.F., Szoka Jr., F.C., 2006. Barriers to carrier mediated drug and gene delivery to brain tumors. J. Control. Release 110, 236–259.

Jung, S.H., Kim, S.K., Jung, S.H., Kim, E.H., Cho, S.H., Jeong, K.-S., Seong, H., Shin, B.C., 2010. Increased stability in plasma and enhanced cellular uptake of thermally denatured albumin-coated liposomes. Colloids Surf. B Biointerfaces 76, 434–440.

Kumagai, A.K., Eisenberg, J., Pardridge, W.M., 1521. Absorptive-mediated endocytosis of cationized albumin and a β-endorphin-cationized albumin chimeric peptide by isolated brain capillaries. J. Biol. Chem. 262, 4–15219.

Lasic, D.D., Ceh, B., Stuart, M.C.A., Guo, L., Frederik, P.M., Barenholz, Y., 1995. Transmembrane gradient driven phase transitions within vesicles: lessons for drug delivery. Biochem. Biophys. Acta 14, 145–156.

Lee, R.J., Low, P.S., 1995. Folate-mediated tumor cell targeting of liposome-entrapped doxorubicin *in vitro*. Biochim. Biophys. Acta 1233, 134–144.

Li, S.-D., Huang, L., 2010. Stealth Nanoparticles: high density but sheddable PEG is a key for tumor targeting. J. Control. Release 145, 178–181.

Liu, L., Guo, K., Lu, J., Venkatraman, S.S., Luo, D., Ng, K.C., Ling, E.-A., Moochhala, S., Yang, Y.-Y., 2008. Biologically active core/shell nanoparticles self-assembled from cholesterol-terminated PEG-TAT for drug delivery across the blood–brain barrier. Biomaterials 29, 1509–1517.

Maeda, N., Takeuchi, Y., Takada, M., Sadzuka, Y., Namba, Y., Oku, N., 2004. Anti-neovascular therapy by use of tumor neovasculature-targeted long-circulating liposome. J. Control. Release 100, 41–52.

Mayer, L.D., Tai, L.C.L., Ko, D.S.C., Masin, D., Ginsberg, R.S., Cullis, P.R., Bally, M.B., 1989. Influence of vesicle size, lipid composition and drug to lipid ratio on the biological activity of liposomal doxorubicin in mice. Cancer Res. 49, 5922–5930.

Ntziachristos, V., Bremer, C., Issleder, R., 2003. Fluorescence imaging with nearinfrared light: new technological advances that enable *in vivo* molecular imaging. Eur. Radiol. 13, 195–208.

Pardridge, W.M., Triguero, D., Buciak, J., 1989. Transport of histone through the blood–brain barrier. J. Pharmacol. Exp. Ther. 251, 821–826.

Petri, B., Bootz, A., Khalansky, A., Hekmatara, T., Müller, R., Uhl, R., Kreuter, J., Gelperina, S., 2007. Chemotherapy of brain tumour using doxorubicin bound to surfactant-coated poly(butyl cyanoacrylate) nanoparticles: revisiting the role of surfactants. J. Control. Release 117, 51–58.

Qin, Y., Chen, H., Yuan, W., Kua, R., Zhang, Q., Xie, F., Zhang, L., Zhang, Z., Liub, J., He, Q., 2011. Liposome formulated with TAT-modified cholesterol for enhancing the brain delivery. Int. J. Pharm., doi:10.1016/j.ijpharm.2011.07.021.

Roney, C., Kulkarni, P., Arora, V., Antich, P., Bonte, F., Wu, A., Mallikarjuana, N.N., Manohar, S., Liang, H.-F., Kulkarni, A.R., Sung, H.-W., Malladi Sairam, D., Aminabhavi, T.M., 2005. Targeted nanoparticles for drug delivery through the blood–brain barrier for Alzheimer's disease. J. Control. Release 108, 193–214.

Santra, S., Yang, H., Stanley, J.T., Holloway, P.H., Moudgil, B.M., Walter, G., 2005. Rapid and effective labeling of brain tissue using TAT-conjugated CdS:Mn/ZnS quantum dots. Chem. Commun. 25, 3144–3146.

Schwarze, S.R., 1999. *In vivo* protein transduction: delivery of a biologically active protein into the mouse. Science 285, 1569–1572.

Sharma, A., Sharma, U.S., 1997. Liposomes in drug delivery: progress and limitations. Int. J. Pharm. 54, 123–140.

Takasato, Y., Rapoport, S.I., Smith, Q.R., 1984. An in situ brain perfusion technique to study cerebrovascular transport in the rat. Am. J. Physiol. 247, 484–493.

Tamai, I., Tsuji, A., 1996. Drug delivery through the blood–brain barrier. Adv. Drug Deliv. Rev. 19, 401–424.

Terasaki, T., Hirai, K., Sato, H., Kang, Y.S., Tsuji, A., 1989. Absorptive-mediated endocytosis of a dynorphinlike analgesic peptide E-2078, into the blood–brain barrier. J. Pharmacol. Exp. Ther. 251, 351–357.

Torchilin, V.P., 2005. Recent advances with liposomes as pharmaceutical carriers. Nat. Rev. Drug Discov. 4, 145–160.

Tromberg, B.J., Pogue, B.W., Paulsen, K.D., Yodh, A.G., Boas, D.A., Cerussi, A.E., 2008. Assessing the future of diffuse optical imaging technologies for breast cancer management. Med. Phys. 35, 2443–2451.

Vives, E., Brodin, P., Lebleu, B., 1997a. A truncated HIV-1 TAT protein basic domain rapidly translocates through the plasma membrane and accumulates in the cell nucleus. J. Biol. Chem. 272, 16010–16017.

Vives, E., Granier, C., Prevot, P., Lebleu, B., 1997b. Structure activity relationship study of the plasma membrane translocating potential of a short peptide from HIV-1 TAT protein. Lett. Pept. Sci. 4, 429–436.

Wender, P.A., Mitchell, D.J., Pattabiraman, K., Pelkey, E.T., Steinman, L., Rothbard, J.B., 2000. The design, synthesis, and evaluation of molecules that enable or enhance cellular uptake: peptoid molecular transporters. Proc. Natl. Acad. Sci. U.S.A. 97, 13003–13008.

William, M., Pardridge, T., 2005. Drug and gene targeting to the brain via blood–brain barrier receptor-mediated transport systems. Int. Congr. Ser. 1277, 49–62.

Xiong, X.-B., Huang, Y., Lu, W.-L., Zhang, X., Zhang, H., Nagai, T., Zhang, Q., 2005. Enhanced intracellular delivery and improved antitumor efficacy of doxorubicin by sterically stabilized liposomes modified with a synthetic RGD mimetic. J. Control. Release 107, 262–275.

Xu, R.X., Young, D.C., Mao, J.J., Povoski, S.P., 2007. A prospective pilot clinical trial evaluating the utility of a dynamic near-infrared imaging device for characterizing suspicious breast lesions. Breast Cancer Res. 9, R88.

Yang, Y., Wang, J., Zhang, X., Lu, W., Zhang, Q., 2009. A novel mixed micelle gel with thermo-sensitive property for the local delivery of docetaxel. J. Control. Release 135, 175–182.

Zhao, X.B., Muthusamy, N., Byrd, J.C., Lee, R.J., 2007. Cholesterol as a bilayer anchor for PEGylation and targeting ligand in folate-receptor-targeted liposomes. J. Pharm. Sci. 9, 2424–2439.